Research Square

Preprints are preliminary reports that have not undergone peer review.
They should not be considered conclusive, used to inform clinical practice,
or referenced by the media as validated information.

Development of an Enhanced Aerial Photogrammetric Process for Precise 3D Model Reconstruction and validation by Volume Calculation

Naveenkumar K

naveen.civil@avit.ac.in

Aarupadai Veedu Institute of Technology, Vinayaka Missions Research Foundation

Ranjith Babu B

PNSA College of Engineering and Technology

Laxmi Alekhya Devathi V N V

Anurag Engineering College

Agnishwar J

CEO, Garuda Aerospace Ltd

Rithika Mohan

CAO, Garuda Aerospace Ltd

Karthikeyan R

VP, Garuda Aerospace Ltd

Research Article

Keywords: Photogrammetry, autonomous drone surveying, non-autonomous image capture, Digital Elevation Models (DEM), and Orthomosaic images

Posted Date: July 30th, 2026

DOI: https://doi.org/10.21203/rs.3.rs-10248883/v1

License: This work is licensed under a Creative Commons Attribution 4.0 International License.
Read Full License

Additional Declarations: No competing interests reported.

Abstract

Photogrammetry-based 3D reconstruction is a suitable technique for creating precise digital models from overlapping photographs. The need of this research is to optimize image acquisition angles so that precise 3D models may be extracted with Agisoft Metashape post-processing software. The goal was to find suitable camera angle combinations that would reduce picture acquisition time and data volume while delivering the maximum operational accuracy. Unlike standard autonomous drone surveying techniques, the proposed methodology used a non-autonomous approach in which photos were manually captured around the object, significantly reducing drone flight time and redundant data collection. To take photographs for proof-of-concept study, a mobile phone camera was initially used, followed by a drone-mounted camera. Photos were shot from a fixed height of five feet at 30°, 45°, 60°, and 90° viewing angles. Photographs of the paper box object were shot around 360°, with provisions set every 30° to acquire images.

The acquired datasets were processed singly and in combined angle sets to produce 3D models, Digital Elevation Models (DEM), and Orthomosaic images. The reliability of the model was confirmed by comparing the estimated object volume resulting from the rebuilt model to the actual object volume measured by conventional method. Of all the setups tested, the combined capture angles of 45° and 60° yielded the most precise and dependable 3D reconstruction. The study concludes that, while creating 3D models, optimal non-autonomous image capture techniques can effectively reduce data requirements while maintaining outstanding photogrammetric accuracy less than 0.5 percentage in the combined post processing of image captured at the angle of 45° and 60°.

1. Introduction

Photogrammetry is the process of reconstructing 3D things from 2D photographs. The technique of 3D mapping relies more on accurate 3D reconstruction. It is process of determining the exact size of the object, particularly with different geometric features. The aim of this experimental investigation is to analyse the performance of angle optimization with the least amount of data while obtaining the required output. It produces 3D reconstructions from photographs captured using a mobile phone camera. This research work uses Agisoft Metashape for post-processing to provide digital elevation model output and QGIS for virtual volume calculation (Enesi et al 2022).

A professional photogrammetry software called Agisoft Metashape processes digital photos photogrammetrically to create 3D spatial data for usage in GIS applications, documentation of cultural assets, creation of visual effects, and indirect measurements of various-sized objects (Enesi et al 2023). The tiled model, point cloud, DEM, orthomosaic, and panorama view are the outputs that the software generates. Agisoft software applies machine learning approaches to post-processing and analytic operations with the goal of producing industry-specific outcomes.

Dense point clouds, textured polygonal models, and georeferenced orthomosaics are examples of high-value spatial information produced by the program from RGB or multispectral camera images, including

multi-camera systems. Additionally, post-processing can automatically identify dense point clouds, compute vegetation indices, extract data for agricultural equipment action maps, and eliminate shadows and texture artifacts from models (Yebin Liu et al 2013, Choi et al 2015, Grant et al 2016).

A single view does not provide sufficient information regarding the 3D shape, considerable traditions are required for 3D reconstruction from collected images, resulting in lower accuracy. However, utilizing either active or passive methods, Multiview techniques can directly observe depth. While passive approaches focus on changes in the signal that the gadget itself emits, active methods send out a signal and analyze how the scene reflects it. This work will focus on the account of passive systems, which just require basic cameras, like those present on mobile devices, as active techniques require specialized hardware (Hanbyul et al 2015, Goldlucke et al 2014, Dehais 2017, Soltani 2017 & Fidji 2020).

Photogrammetry is a technique for creating 3D models from images of physical objects in various locations, probably while the object at rest (Tatarchenko et al 2019). It operates by taking 2D data around the object at different viewing angle as placing well as static angle. Since the objects vary in size, photogrammetry applications generate the geospatial features like point cloud of the object to be analysed for the purpose of 3D model (Marian et al 2021, Hartley et al 2023, Newcombe 2011 & Zhu 2017).

Using volume-to-volume translation CNN, a 3D model was generated from RGB photos. A rich semantic representation derived from the SMPL model has been suggested as an additional input to address the uncertainties related to surface geometry reconstruction, including the reconstruction of invisible areas (Dai 2017 and Maier et al 2017). Because of its ability to obtain colour (RGB) and depth information in real time, RGB-D sensors like Microsoft Kinect, Intel RealSense, and Google Tango have drawn a lot of interest in the fields of computer vision, robotic perception, and 3D surface reconstruction. As a result, volumetric fusion techniques have proven to be highly effective in producing accurate and dense 3D surface models from noisy RGB-D sensor data (Alldieck et al 2018).

These RGB-D sensors are inexpensive, which drives research in dense 3D mapping and scene reconstruction, even with depth uncertainty, terrain sensor noise, missing data, and low spatial resolution. To merge the existing data shortcomings, researchers proposed new reconstruction methods using volumetric fusion and depth-frame integration methods, which allow the combination of multiple depth-dependent image frames into one volume (Lee et al 2010 & Yu 2013). By merging redundant depth readings for multiple views (Zeng Huang et al 2018), the methods noticeably reduce random noise, and improve geometric consistency and surface smoothness.

To achieve accurate 3D reconstruction, Calibrated cameras with known intrinsic and extrinsic parameters take many overlapping images to perform an accurate 3D reconstruction. Using stereo vision techniques (Steinbruecker et al 2013 & Zuza 2013), object geometry is reconstructed from images of an object taken from multiple viewpoints as features are matched across the images using epipolar geometry and triangulation to compute 3D coordinates.

Shape-from-silhouette or space-carving techniques (Nießner et al 2013) also reconstruct object shapes from segmented, 2D silhouettes collected from multiple, pre-aligned viewpoints. The silhouettes are cast

into a three-dimensional space, and incomplete regions are removed to form the object's visual hull and a 3D surface representation.

2. Methodology

The angle of view (AoV) on the object is at 30°, 45°, 60°, and 90° twelve images were taken. The horizontal ground angle was kept constant at 30° between subsequent image takes. A total of 12 images per viewing angle configuration were captured due to a full 360° at every 30° location for a single trail. For each trial the camera orientation was adjusted to provide the required viewing angle, while keeping the pre-determined angular interval around the object to be mapped. The procedure for validation of the obtained 3D models is presented in Fig. 1.

Images were captured from four different viewing angles such as 30°, 45°, 60°, and 90° at the constant height of 5 feet. The AoV is the camera's perspective relative to the object. Between each sequential shot, the horizontal ground angle was constrained to 30°. The images were captured at the ground angle in twelve set location completing a 360°. The position of the image capture setup was adjusted for each image capture to set the required viewing angle while keeping the pre-determined angle of interval around the object. An example of the procedure for verifying the completed 3D models is shown in Fig. 1.

To find the precision and accuracy of the 3D models generated virtually, the collected image datasets were distinctly processed and also in combination by using Agisoft Metashape software. The final results will generate a Digital Elevation Model (DEM) and an orthomosaic image. The volume will be calculated within the program environment by processing the Digital Elevation Model with QGIS. The computed volume will then be compared to the manually measured volume to ensure the precision of the obtained 3D model and DEM.

2.1 Utilization of materials and Landscape of the Venue

The experiment to determine the optimal viewing angle was carried out on a flat surface inside the Garuda Aerospace facility. Initially, a circle was drawn and divided into 12 equal parts spaced 30 degrees apart. Photographs were taken at 30° intervals around the whole 360° circumference, with a constant height of 5 feet and a flat surface throughout the experiment. All pictures used for angle optimization in photogrammetry were taken with a mobile phone camera (Kraus 2017).

After angle optimization, a quadcopter UAV manufactured by Garuda Aerospace Limited (Table 1) is deployed to capture photos. The acquired data is then processed to generate a DEM and an orthomosaic image to validate the proposed methods for generating a 3D model of the object.

Table 1
Specifications of UAVs and RGB Camera Specifications

S. No	UAV	Specifications	RGB Camera	Specifications
1	Weight	1380 g	Camera Resolution	21 Megapixels
2	Flight Altitude	Max. 15 metres	Image Resolution	5472 × 3648 pixels
3	Flight Time	Max. 10 minutes	Focal Length	9 mm
4	Speed	Max. 8 m/s (For Autonomous flight) Max. 5 m/s (For Manual flight)	Sensor Width	1200 mm
5	Maximum Wind Resistance	10 m/s	Image Acquisition Device	UAV-mounted Camera

3. Experimental Analysis

Initially, three control points were marked, and the distances between them were measured with higher accuracy. The object was then positioned within the designated control points. Subsequently, the photogrammetric process was executed by utilizing the recommended manual operation methodology. Figure 2 depicts the experimental setup for acquiring photographs for the photogrammetry procedure.

The differential global positioning system (DGPS) equipment, Trimble R8s receiver, was used to measure latitude and longitude coordinates for drone picture acquisition using photogrammetric methods. Table 2 shows the Trimble R8s receiver's specifications.

Table 2. Specifications of the DGPS Trimble R8s

S. No	Description	Specifications
1	Receiver Type	GNSS RTK Receiver
2	Channels	440 channels with Trimble Maxwell 6 custom survey GNSS chips
3	Satellite Tracking	GPS, GLONASS, Galileo, BeiDou, and QZSS
4	Static Survey Accuracy	Horizontal: ± (3 mm + 0.5 ppm) RMS Vertical: ± (5 mm + 0.5 ppm) RMS
5	RTK Accuracy	Horizontal: ± (8 mm + 1 ppm) RMS Vertical: ± (15 mm + 1 ppm) RMS
6	PPK Accuracy	Horizontal: ± (8 mm + 1 ppm) RMS Vertical: ± (15 mm + 1 ppm) RMS
7	Communication	Bluetooth, GSM/GPRS/EDGE/UMTS /HSPA+, UHF Radio

3.1 Camera Angle and Post-Processing Methodology

The current study uses frame-to-model tracking for 3D reconstruction, in which the camera pose of each incoming image frame is continually assessed in relation to an already constructed sparse or dense 3D reference model. This method allows for real-time localization and mapping by identifying the six degrees of freedom (6-DoF) of each collected frame, specifically the translation and rotation parameters. All captured image frames are subjected to depth analysis in order to quantify the spatial distance of object surfaces from the camera perspective (Or-El et al 2015 & Asadpour et al 2021).

Stereo matching, multi-view geometry, and Structure-from-Motion (SfM) approaches are used to estimate depth by computing three-dimensional coordinates using parallax differences between overlapping pictures. Dense image matching algorithms are then used to create a detailed point cloud visualization of the object's surface. The point cloud is made up of millions of geographically referenced XYZ coordinates that precisely define the object's geometry, texture, and surface features (Wu et al 2014, Novotny et al 2018 & Schonberger et al 2016).

Single image-based reconstruction approaches can be utilized to recreate 3D shapes by analysing distinct frames separately and then combining them using registration techniques. Ideally, the spatio-temporal correlations between the frames to resolve ambiguities is used, particularly in the presence of occlusions and densely packed scenes. The challenge of processing sequential data has been solved by employing Recurrent Neural Networks (RNN) and Long-Short Term Memory (LSTM) networks, which allow networks to remember their inputs across time (Federica Bogo et al 2016, Jeon et al 2016, Qi et al 2017 & Erich et al 2022).

3.2 Generation of Orthomosaic image and Digital Elevation Model (DEM)

Post data collection, the photos were processed with the Agisoft Metashape software. Initially, image alignment was used to create the 3D model framework. Then, texture mapping, tiled model generation, and dense point cloud assembly were performed. Based on the generated point cloud data DEM, the legible orthophotos indicate explicit geometric evidence of a paper box (Figure 3).

3.3 Calculation of solid volume and validation of 3D Model

The volume computation of a solids is needed in determining the correctness of post-processing outputs. In this study, a three-dimensional (3D) model of rectangular paper and a wooden box was developed. The process employs a mobile camera and aerial vehicle (UAV). To generate an appropriate 3D model, vertical and high-oblique pictures (0°, 30°, 45°, 60°, and 90°) were captured at a constant height of 5 feet in case of mobile camera utilization and for UAV altitude is fixed at 30 feet.

The solid volume was determined by uploading and processing the DEM using the QGIS 3.44.6 software. Using established volume calculation methods, such as traditional raster or section methods in software, the volume of solids is computed. Despite the limitations, such as the high level of work required or the low calculation accuracy, the conversional method of volume computation is utilized for validation purposes. The object manually measured volume is calculated to be 0.00189 m^3. The angle is optimized depending on the calculation of error between manually measured volume and volume measured in software (Table 3).

Table 3. Angle optimization and Computation of error in volume calculation

Photograph Taken by (Mobile Cam/Drone)	Angle & Height of the Photograph Taken	Ortho mosaic Image	DEM	Remarks
Mobile Cam	0 degree & Constant (5 feet in the mobile cam)	-	-	• The Ground control points partially not able match and difficult to process the images in software due to less Ground control points. • Able to get only the height of the Box only less details about the box.
Mobile Cam	30 degree & Constant (5 feet in the mobile cam)			• Got all the details (Length, Breath and Depth) • Able to calculate Volume (0.00207 m^3). • + 9.52 % Error in volume.
Mobile Cam	45 degree & Constant (5 feet in the mobile cam)			• Able to get all the details (Length, Breath and Depth). • Able to calculate Volume (0.00211 m^3). • + 11.64 % Error in volume.
Mobile Cam	60 degree & Constant (5 feet in the mobile cam)			• Able to get all the details (Length, Breath and Depth). • Able to calculate Volume (0.00143 m^3). • - 24.34 % Error in volume.
Mobile Cam	0,30,45 degree & Constant (5 feet in the mobile cam)			• Able to get all the details (Length, Breath and Depth). • Able to calculate Volume (0.00140 m^3). • - 25.90 % Error in volume.
Mobile Cam	0,30,45,60,90 degree & Constant (5 feet in the mobile cam)			• Able to get all the details (Length, Breath and Depth). • Able to calculate Volume (0.00345 m^3). • + 82.5 % Error got in volume.
Mobile Cam	30,45 degree & Constant (5 feet in the mobile cam)			• Able to get all the details (Length, Breath and Depth). • Able to calculate Volume (0.00423 m^3). • + 123.8 % Error in volume.

Mobile Cam	60,90 degree & Constant (5 feet in the mobile cam)			• Able to get all the details (Length, Breath and Depth). • Able to calculate Volume (0.00201 m^3). • + 6.35 % Error in volume.
Mobile Cam	30,60 degree & Constant (5 feet in the mobile cam)			• Able to get all the details (Length, Breath and Depth). • Able to calculate Volume (0.00158 m^3). • + 16.40 % Error in volume.
Mobile Cam	45,90 degree & Constant (5 feet in the mobile cam)			• Able to get all the details (Length, Breath and Depth). • Able to calculate Volume (0.00297 m^3). • + 57.14 % Error in volume.
Mobile Cam	30,90 degree & Constant (5 feet in the mobile cam)			• Able to get all the details (Length, Breath and Depth). • Able to calculate Volume (0.00337 m^3). • + 78.31 % Error in volume.
Mobile Cam	90 degree & Constant (5 feet in the mobile cam)			• Able to get all the details (Length, Breath and Depth). • Able to calculate Volume (0.00182 m^3). • - 3.70 % Error in volume.
Mobile Cam	30,45,60 degree & Constant (5 feet in the mobile cam)			• Able to get all the details (Length, Breath and Depth). • Able to calculate Volume (0.00195 m^3). • + 3.18 % Error in volume.
Mobile Cam	**45,60 degree & Constant (5 feet in the mobile cam)**			• **Able to get all the details (Length, Breath and Depth).** • **Able to calculate Volume (0.00190 m^3).** • **+ 0.53 % Error in volume.**

Using 30°, 45°, and 60° picture acquisition angles at a constant height of 5 feet yielded entire object details and a computed volume of 0.00195 m³ with a +3.18% error. Using a 45° and 60° angle combination at the same height improved accuracy, resulting in a volume of 0.00190 m³ with a +0.53% inaccuracy. Image capture at 90° yielded complete object information, but resulted in a computed volume of 0.00182 m³ with a -3.70% inaccuracy. Among all of the image capture configurations studied, the combination of 45° and 60° angles resulted in the highest accurate volume estimation and 3D model validation.

3.4 Agisoft Metashape Software

The assessment of actual object for 3D reconstruction is discussed in this session. Agisoft Metashape will be used to recreate the object in three dimensions. Improved reconstruction is made possible by increasing the number of pictures taken for processing. The rebuilt object is a scaled-down duplication of the original. A known size element is needed in order to acquire the actual dimensions. It is possible to obtain the object in its actual size and measure its other dimensions by rescaling the rebuilt item using the known dimension. The 3D reconstruction is scaled using the target object's known size. Markers are specified, and the scale among them is determined. To achieve the best outcomes, markers are established along three axes.

3.4.1 Image processing in Agisoft Metashape Software

The captured images for photogrammetric processing were uploaded to Agisoft Metashape utilizing the workflow menu's "Add Photos/Add Folder" option. After importing the photographs, the photo alignment method (camera alignment) was used to determine the spatial relationship of the collected images. During this stage, essential parameters such feature point recognition, picture matching, and camera position estimation were improved to increase photogrammetric reconstruction accuracy. Figure 2 depicts three markers, together with their specifications.

3.4.2 Tie Points Limit

The current method results in 20,986 tie points (Figure 3), which is the highest number of points that Agisoft will match between photographs in this case; the default is 4000. Enhancing this value results in more accuracy but requires hours of processing. Key points are immediately identifiable elements of interest in the photographs, such as great contrast or fascinating texture. The number of important points varies depending on the size of the photographs and their visual substance.

3.4.3 Generation of Tiled model and Point Cloud

To enhance the quality and accuracy of the 3D reconstruction, images were aligned, resulting in a dense point cloud and tiled model. The dense point cloud is formed by representing the object surface with a large number of spatial points, which aids in collecting detailed geometry and surface information. The tiled model is generated to obtain a high-resolution 3D image with optimum texture mapping and efficient display of complex surfaces (Figure 4).

These results are essential for the generation of an accurate DEM, Orthomosaics, volume calculations and for the relative accuracy assessment of the photogrammetric model. The dense point cloud has a higher number of spatial coordinate points for the exact representation of the object’s geometry and surface characteristics. This complete geographical information is used to generate the Digital Elevation Model (DEM) that uses surface points to capture the variation of the terrain and the heights of the objects.

An orthomosaic image obtained from the point cloud matches the positions of the cameras in this assessment. The process of applying geometric correction to image by mending together several aligned

images generates a 1,271,256 point clouds and the faultless image with spatial accuracy is shown in (Figure 5).

3.5 QGIS Software

The Digital Elevation Model (DEM) was generated in Agisoft Metashape and then imported into QGIS version 3.44.6 for volume analysis. After importing the DEM, an additional reference layer was built and assigned an appropriate base elevation value in order to process the DEM correctly. The volume was then estimated from the DEM data using QGIS' "Raster Surface Volume" tool (Figure 6). The computed volume acquired using QGIS was then compared to the manually estimated volume to determine the correctness and validity of the photogrammetric reconstruction technique.

4 Validation of Optimized Image Acquisition Angles Using Aerial Photogrammetry

The image acquisition angle was tuned to determine the viewing configuration that resulted in the lowest error in photogrammetric reconstruction and volume estimate. After establishing the optimal angle combination, the same photogrammetric process was used for additional confirmation. Although the general technique remained constant, the experimental equipment and research location were changed (Fig. 7). Instead of employing a mobile camera for terrestrial picture acquisition, a drone was used to execute the aerial photogrammetry (Wu et al 2013, Akgul et al 2018, Andrew Gilbert et al 2018).

The use of aerial photogrammetry improved image coverage, increased overlap between successive images, and improved surface visibility from numerous perspectives. These characteristics resulted in less occlusion and improved feature matching, camera alignment and dense point cloud generation across the different stages of photogrammetric processing. Aerial imagery acquired with a drone was processed in Agisoft Metashape to produce an orthomosaic, 3D models, a dense point cloud and a Digital Elevation Model (DEM). The DEM was imported into QGIS and the Raster Surface Volume tool was used to estimate volume. The error between the estimated and calculated volume is less than 2.76 percent.

The obtained results have shown that the corrected image acquisition angles lead to accurate results in the aerial photogrammetry. The estimated volume values were very close to the values obtained from manual measurements, which indicates that the proposed improved angle configuration is effective for terrestrial and aerial photogrammetry. Moreover, the drone-based method has improved the efficiency of data collection, the spatial coverage and consistency of image capture, leading to increased overall reliability and correctness of the 3D reconstruction process.

Conclusion

In this research, we used photogrammetric techniques to determine the optimum angles for capturing images to generate accurate 3D models and estimate volumes with high accuracy. The images as been captured from various angles including 0°, 30°, 45°, 60°, and 90°. The image processing is done in Agisoft Metashape software to generate dense point clouds, tiled models, Digital Elevation Models (DEM), and

orthomosaic images. We analysed the resulting DEMs using QGIS software with the Raster Surface Volume tool to estimate volume.

The experimental findings demonstrated that the quality and accuracy of photogrammetric reconstruction are significantly impacted by the camera viewing angle. The best outcomes for all tested configurations occurred at viewing angles of 45° and 60°, with a volume estimation error of just + 0.53%. The results for 30°, 45°, and 60° also had a smaller inaccuracy of + 3.18%. In contrast, capturing images at 0° led to poor reconstruction because of low feature matching and limited surface visibility.

The study confirmed that using oblique images improves visibility of features, enhances image overlap, and generates dense point clouds. This, in turn, leads to better accuracy in generating digital elevation models (DEMs) and 3D reconstructions. The optimized angle setup was also tested with UAV-based aerial photogrammetry. Aerial images captured by drones provided highly accurate volume estimates. In summary, the study showed that using 45° and 60° viewing angles is the best way to achieve accurate 3D reconstruction and volume estimation for both terrestrial and aerial photogrammetry.

Declarations

Funding Declaration

This research did not receive any specific grant from funding agencies in the public, commercial, or not-for-profit sectors. Garuda Aerospace provided in-kind support to the AICTE Industry Fellowship Programme, including the drone platform and research site for this study.

Data availability

The datasets used and/or analysed in the current study are not publicly available due to institutional and project-related restrictions, but they are available from the corresponding author and Garuda Aerospace Limited upon reasonable request and with permission from the relevant project stakeholders, as applicable.

Competing Interest declaration

The authors have declared that they have no competing interests.

Author Contribution

All authors whose names appear on the submission made substantial contributions to the conception or design of the work; or the acquisition, analysis, or interpretation of data; or the creation of new software used in the work; drafted the work or revised it critically for important intellectual content; approved the version to be published; and agree to be accountable for all aspects of the work in ensuring that questions related to the accuracy or integrity of any part of the work are appropriately investigated and resolved.

Acknowledgement

The authors gratefully acknowledge Garuda Aerospace Private Limited for providing the unmanned aerial vehicle (UAV), access to the survey location, and technical support required to conduct the field investigations under the AICTE Industry Fellowship Programme.

References

1. Akgul M, Yurtseven H, Gulci S, Akay AE (2018) Evaluation of UAV- and GNSS-based DEMs for earthwork volume. Arab J Sci Eng 43:1893–1909
2. Gilbert A, Volino M, Collomosse J, Hilton A (2018) Volumetric performance capture from minimal camera viewpoints. In *Proceedings of the European Conference on Computer Vision (ECCV)* (pp. 591–607)
3. Asadpour A (2021) Documenting historic tileworks using smartphone-based photogrammetry. Mersin Photogrammetry J 3:15–20. https://doi.org/10.53093/mephoj.899432
4. Alldieck T, Magnor MA, Xu W, Theobalt C, Pons-Moll G (2018) Detailed human avatars from monocular video. In *Proceedings of the International Conference on 3D Vision (3DV).*
5. Choi S, Zhou Q-Y, Koltun V (2015) Robust reconstruction of indoor scenes. In *Proceedings of the IEEE Conference on Computer Vision and Pattern Recognition (CVPR).*
6. Creative Tools (n.d.). *Agisoft Metashape*. https://www.creativetools.se/software/metashape
7. Dai A, Nießner M, Zollhöfer M, Izadi S, Theobalt C (2017) Bundle Fusion: Real-time globally consistent 3D reconstruction using on-the-fly surface reintegration. ACM Transactions on Graphics
8. Dehais J, Anthimopoulos M, Shevchik S, Mougiakakou S (2017) Two-view 3D reconstruction for food volume estimation. IEEE Trans Multimedia 19(5):1090–1099. https://doi.org/10.1109/TMM.2016.2642792
9. Enesi I, Kuqi A (2022) Analysing the measurement accuracy of 3D reconstruction for small objects using different software: A case study. J Eng Res Sci 1(12):9–14
10. Enesi I, Kuqi A (2023) Performance analysis for 3D reconstruction objects in Meshroom and Agisoft: A comparative study. Int J Online Biomedical Eng, *22*(5)
11. Erich S, Oto H, Kučera E (2022) Low-cost method for 3D body measurement based on photogrammetry using smartphone. Electronics 11:1048. https://doi.org/10.3390/electronics11071048
12. Fidji B, Yann B (2020) Scyland3D: Processing 3D landmarks. J Open Source Softw 5:1262. https://doi.org/10.21105/joss.01262
13. Bogo F, Kanazawa A, Lassner C, Gehler P, Romero J, Black MJ (2016) Keep it SMPL: Automatic estimation of 3D human pose and shape from a single image. In *Proceedings of the European Conference on Computer Vision (ECCV)* (pp. 561–578)
14. Jeon J, Jung Y, Kim H, Lee S (2016) Texture map generation for 3D reconstructed scenes. Visual Comput 32(6):955–965

15. Goldluecke B, Aubry M, Kolev K, Cremers D (2014) A super-resolution framework for high-accuracy Multiview reconstruction. Int J Comput Vision 106(2):172–191
16. Grant E, Kohli P, van Gerven M (2016) Deep disentangled representations for volumetric reconstruction. In *Proceedings of the European Conference on Computer Vision (ECCV)* (pp. 266–279)
17. Joo H, Liu H, Tan L, Gui L, Nabbe B, Matthews I, Kanade T, Nobuhara S, Sheikh Y (2015) Panoptic studio: A massively multiview system for social motion capture. In *Proceedings of the IEEE International Conference on Computer Vision (ICCV)* (pp. 3334–3342)
18. Hartley R, Zisserman A (2003) Multiple view geometry in computer vision, 2nd edn. Cambridge University Press
19. Marian M, Krajcovic M, Gabajova G (2021) Creating 3D models of transportation vehicles using photogrammetry. Transp Res Procedia 55:584–591. https://doi.org/10.1016/j.trpro.2021.07.025
20. Kraus K (2017) Photogrammetry: Geometry from images and laser scans. Walter de Gruyter
21. Lee H, Won H (2010) Bundle block adjustment with 3D natural cubic splines. Sensors 9:9629–9665. https://doi.org/10.3390/s91209629
22. Maier R, Kim K, Cremers D, Kautz J, Nießner M (2017) Intrinsic3D: High-quality 3D reconstruction by joint appearance and geometry optimization with spatially varying lighting. *arXiv*. https://arxiv.org/abs/1708.01670
23. Newcombe R, Davison A, Izadi S, Kohli P, Hilliges O, Shotton J, Molyneaux D, Hodges S, Kim D, Fitzgibbon A (2011) KinectFusion: Real-time dense surface mapping and tracking. In *Proceedings of the IEEE International Symposium on Mixed and Augmented Reality (ISMAR)*.
24. Nießner M, Zollhöfer M, Izadi S, Stamminger M (2013) Real-time 3D reconstruction at scale using voxel hashing. ACM Trans Graphics, *32*(6), Article 169.
25. Novotny D, Larlus D, Vedaldi A (2018) Capturing the geometry of object categories from video supervision. IEEE Trans Pattern Anal Mach Intell
26. Or-El R, Rosman G, Wetzler A, Kimmel R, Bruckstein AM (2015) RGBD-Fusion: Real-time high precision depth recovery. In *Proceedings of the IEEE Conference on Computer Vision and Pattern Recognition (CVPR)* (pp. 5407–5416)
27. Qi CR, Su H, Mo K, Guibas LJ (2017) PointNet: Deep learning on point sets for 3D classification and segmentation. In *Proceedings of the IEEE Conference on Computer Vision and Pattern Recognition (CVPR)* (pp. 652–660)
28. Schönberger JL, Frahm J-M (2016) Structure-from-motion revisited. In *Proceedings of the IEEE Conference on Computer Vision and Pattern Recognition (CVPR)* (pp. 4104–4113)
29. Soltani AA, Huang H, Wu J, Kulkarni TD, Tenenbaum JB (2017) Synthesizing 3D shapes via modeling multi-view depth maps and silhouettes with deep generative networks. In *Proceedings of the IEEE Conference on Computer Vision and Pattern Recognition (CVPR)* (pp. 1511–1519)
30. Steinbrücker F, Kerl C, Sturm J, Cremers D (2013) Large-scale multi-resolution surface reconstruction from RGB-D sequences. In *Proceedings of the IEEE International Conference on Computer Vision (ICCV)*.

31. Tatarchenko M, Richter SR, Ranftl R, Li Z, Koltun V, Brox T (2019) What do single-view 3D reconstruction networks learn? In *Proceedings of the IEEE/CVF Conference on Computer Vision and Pattern Recognition (CVPR).*
32. Wu C, Stoll C, Valgaerts L, Theobalt C (2013) On-set performance capture of multiple actors with a stereo camera. ACM Trans Graphics, *32*(6), Article 161.
33. Wu C, Zollhöfer M, Nießner M, Stamminger M, Izadi S, Theobalt C (2014) Real-time shading-based refinement for consumer depth cameras. ACM Transactions on Graphics
34. Yu L-F, Yeung S-K, Tai Y-W, Lin S (2013) Shading-based shape refinement of RGB-D images. In *Proceedings of the IEEE Conference on Computer Vision and Pattern Recognition (CVPR)* (pp. 1415–1422)
35. Liu Y, Gall J, Stoll C, Dai Q, Seidel HP, Theobalt C (2013) Markerless motion capture of multiple characters using multiview image segmentation. IEEE Trans Pattern Anal Mach Intell 35(11):2720–2735
36. Huang Z, Li T, Chen W, Zhao Y, Xing J, LeGendre C, Luo L, Ma C, Li H (2018) Deep volumetric video from very sparse multi-view performance capture. In *Proceedings of the European Conference on Computer Vision (ECCV)* (pp. 351–369)
37. Zhu H, Liu Y, Fan J, Dai Q, Cao X (2017) Video-based outdoor human reconstruction. IEEE Trans Circuits Syst Video Technol 27(4):760–770
38. Zuza M (2018) Photogrammetry 2–3D scanning simpler, better than ever. Prusa Printers Blog. https://blog.prusaprinters.org/photogrammetry-23d-scanning-simpler-better-than-ever_29393/

Figures

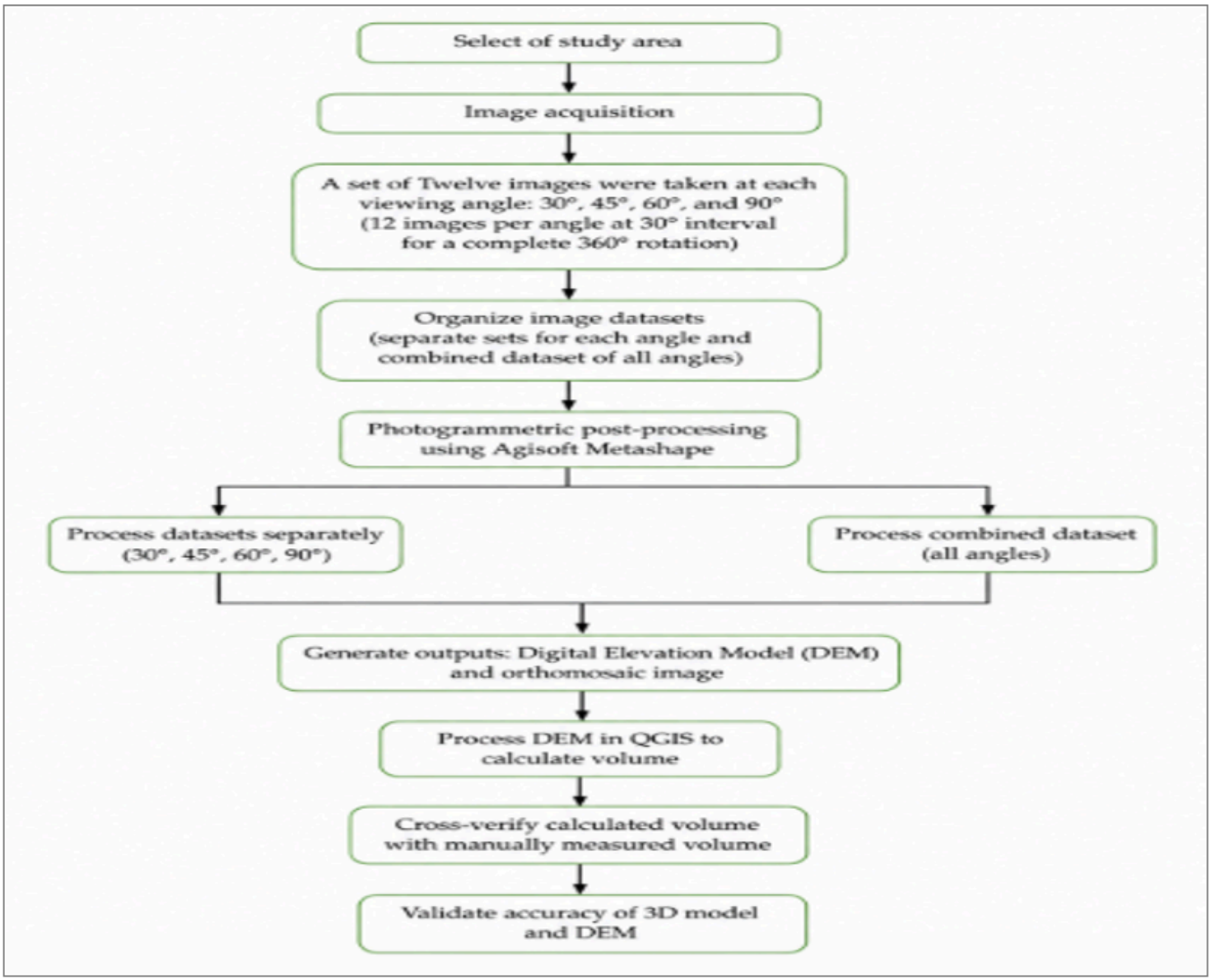

Figure 1

Validating Methodology for 3D Model of object

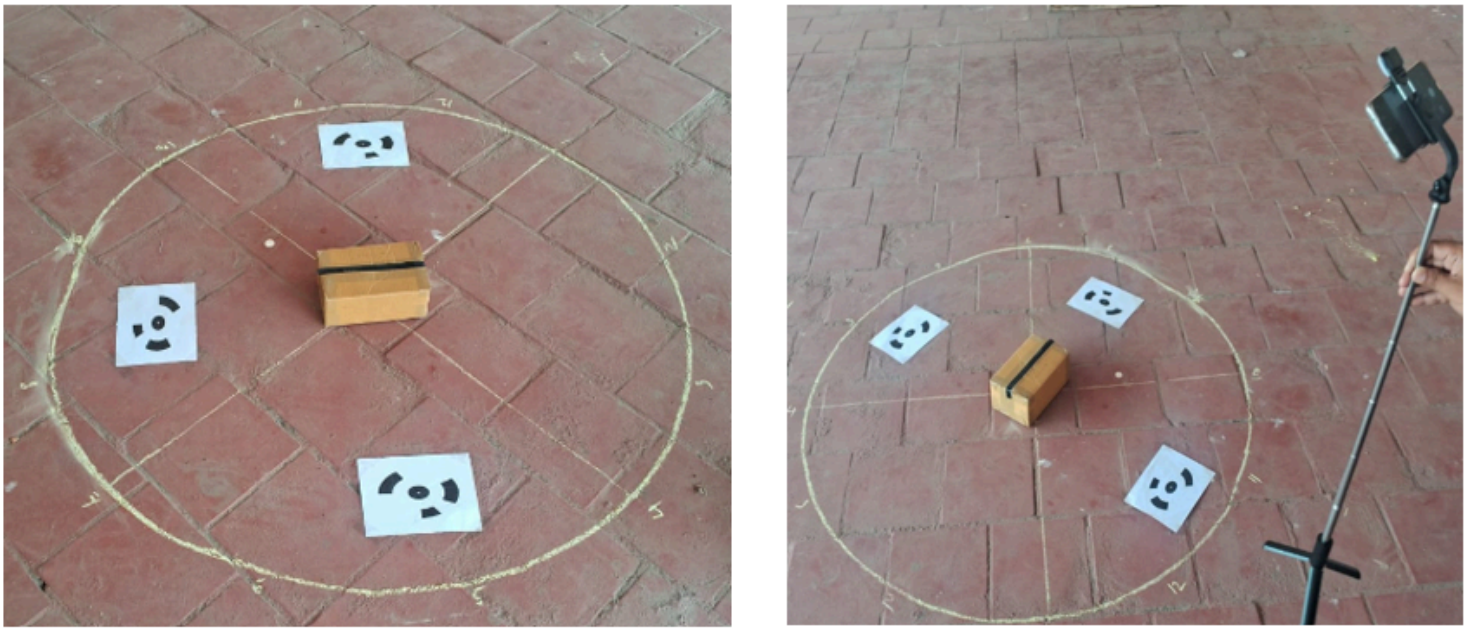

Figure 2

Experimental configuration for photogrammetric 3D reconstruction

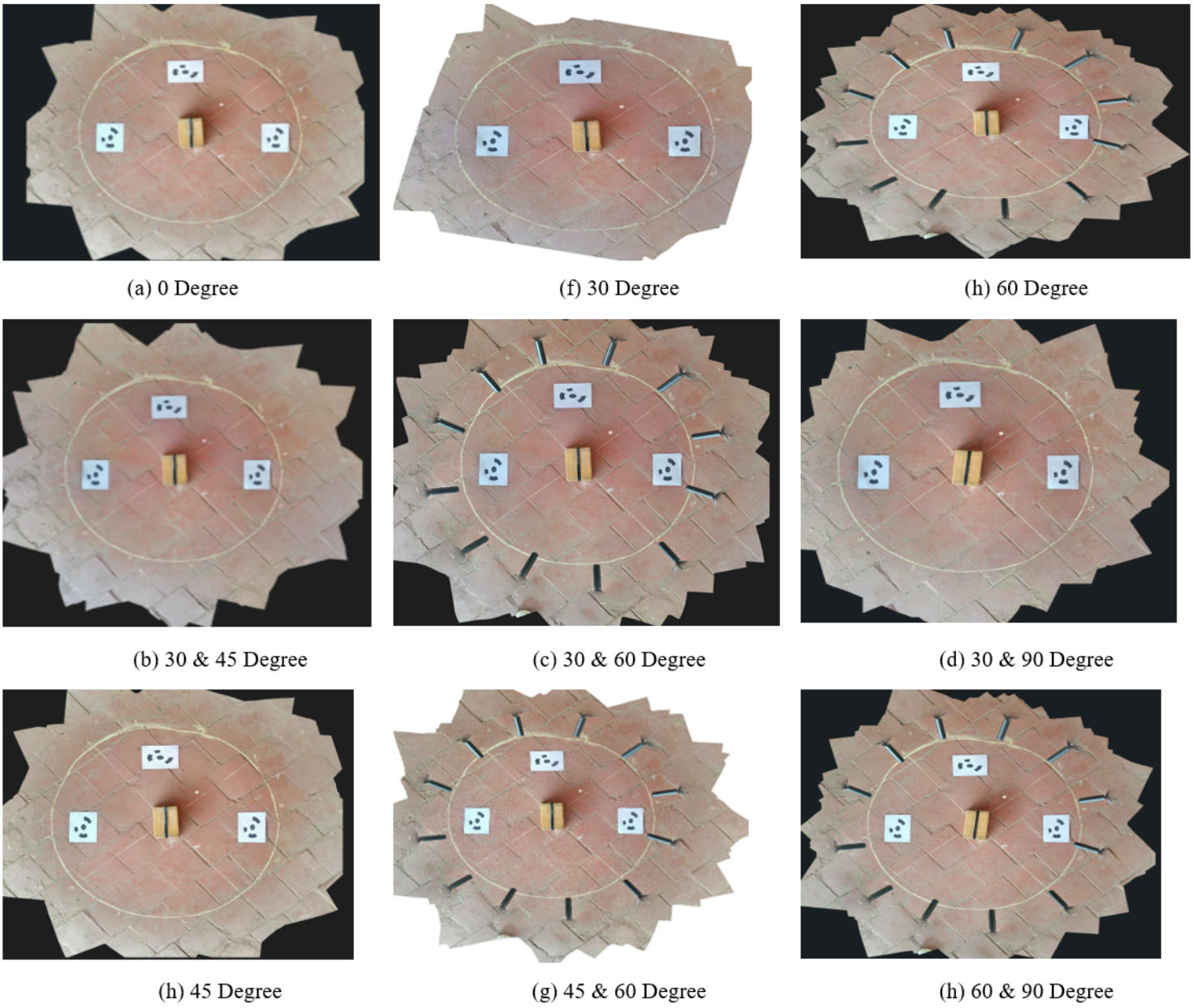

Figure 3

Digital Elevation Model (DEM) and Orthomosaic image



Figure 4

Figure 2. Markers placement in specific 3D positions

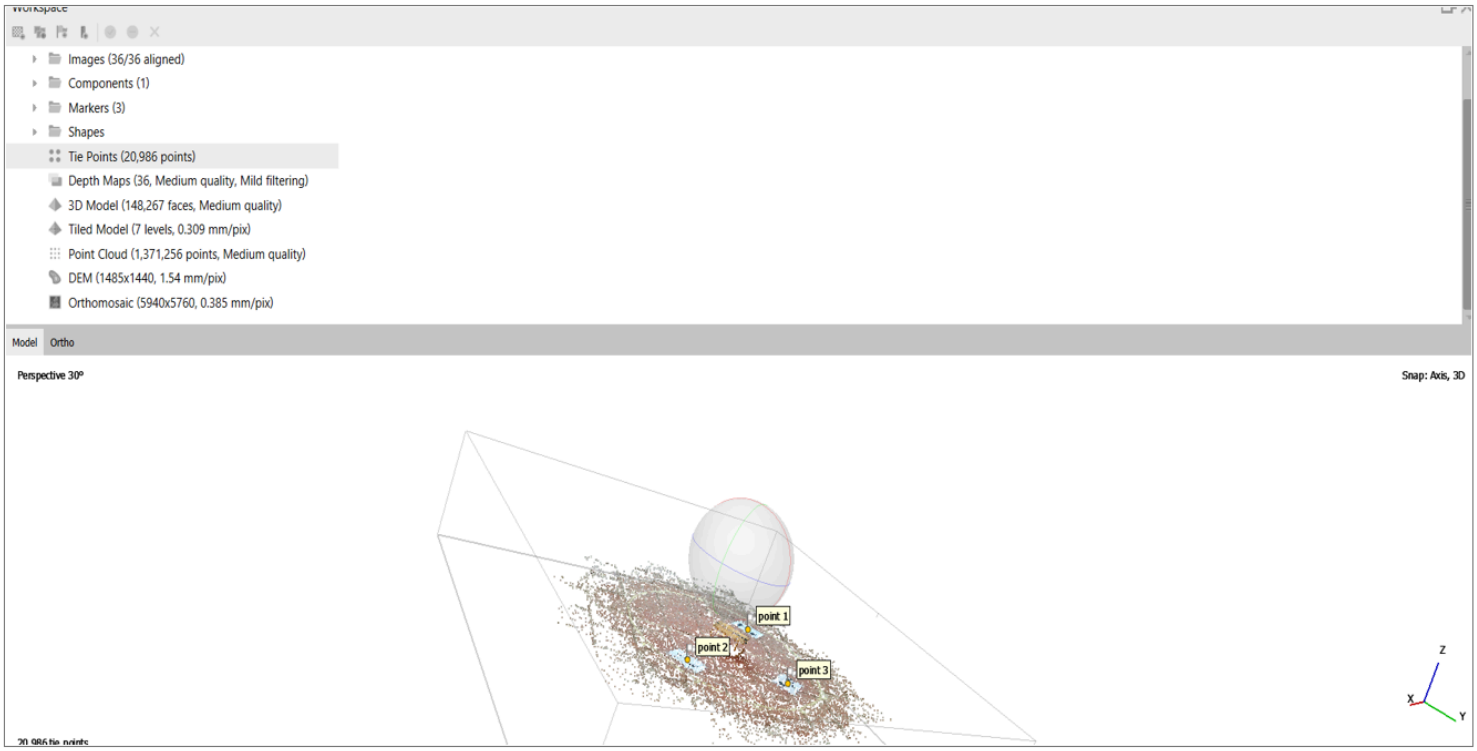

Figure 5

Figure 3. The results of generated Tie Points

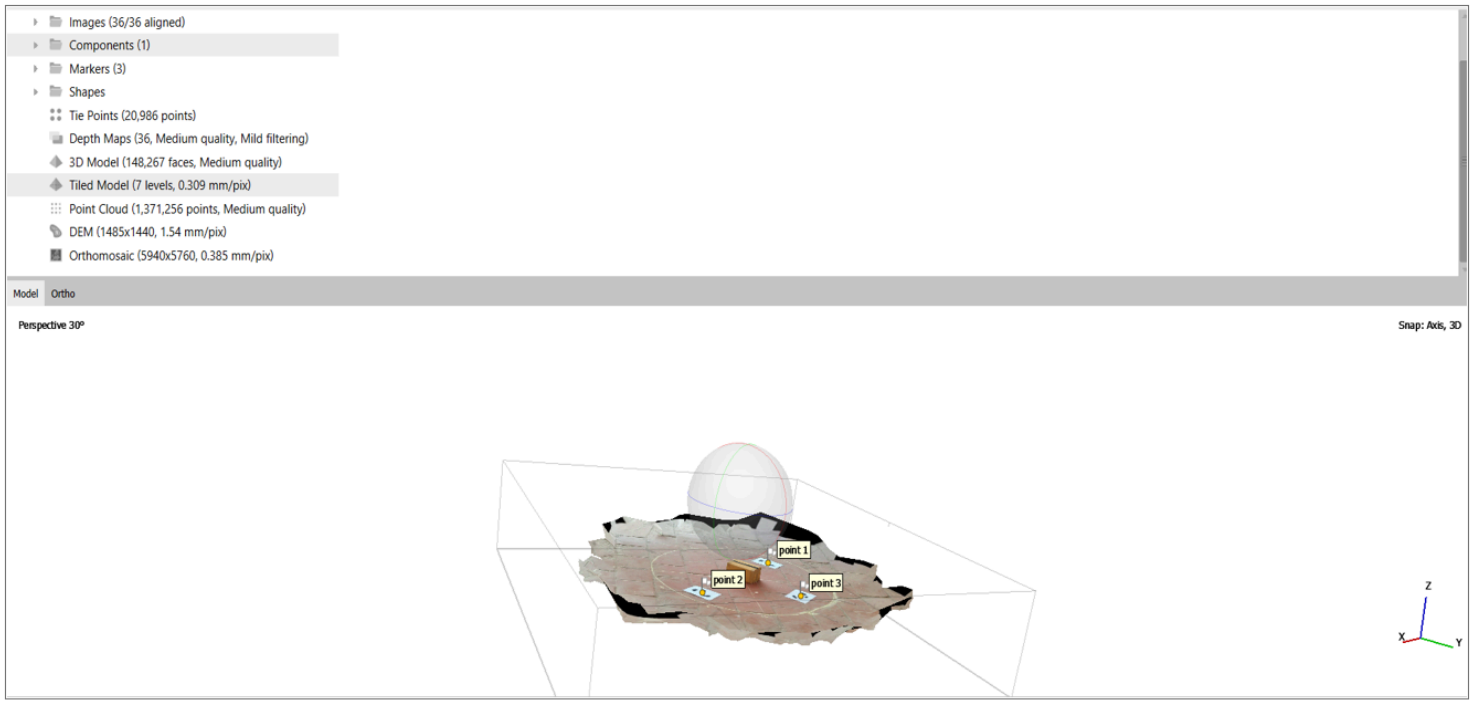

Figure 6

Figure 4. Projection of Tiled Model

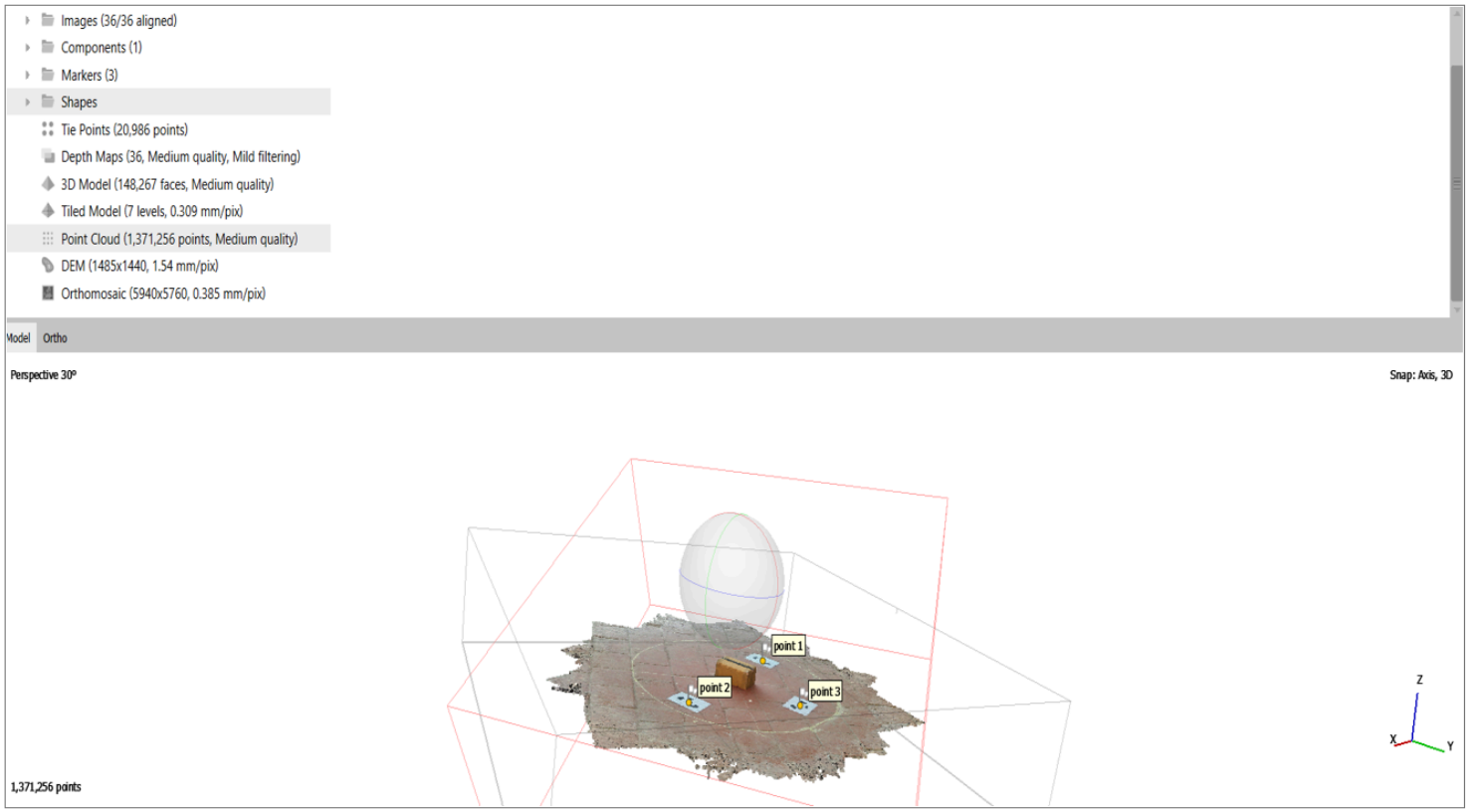

Figure 7

Figure 5. Projection of Point Cloud Model

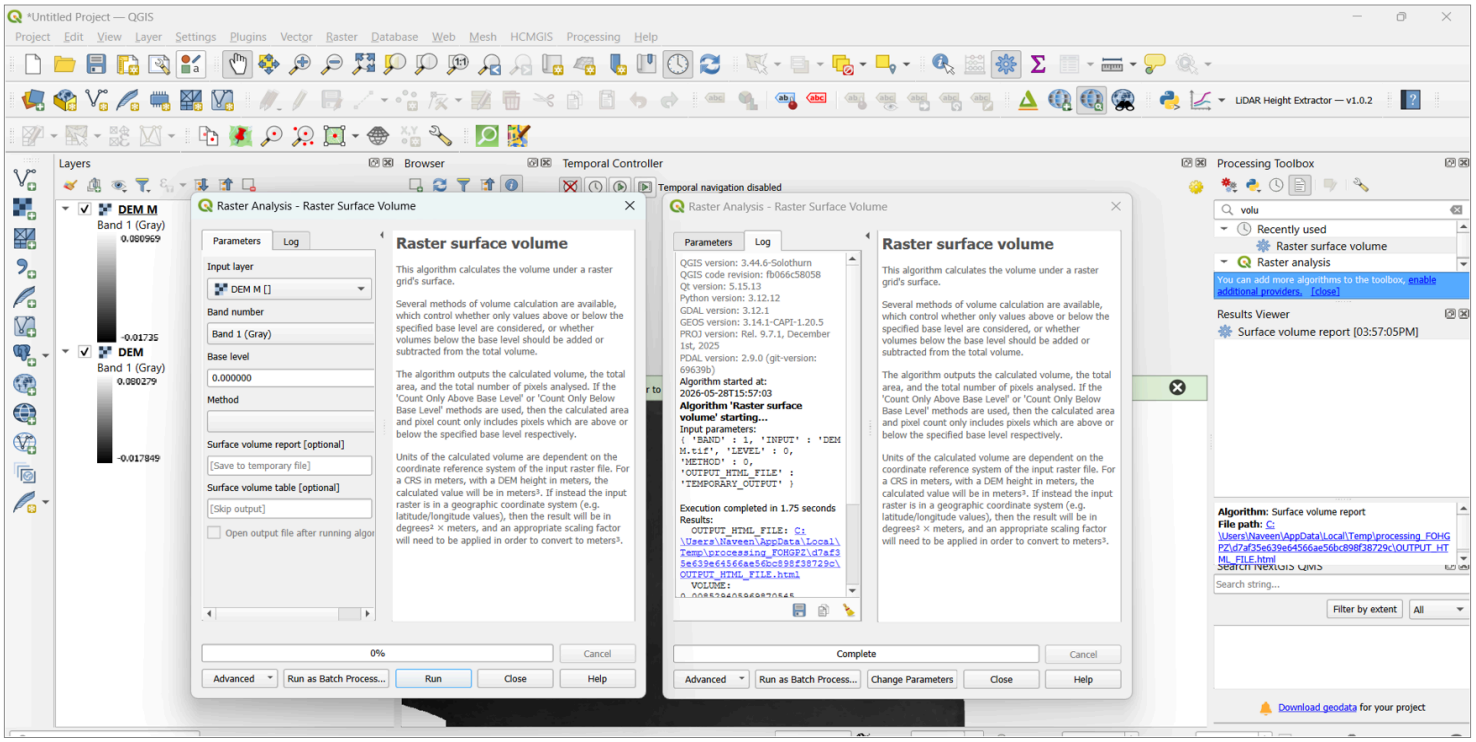

Figure 8

Figure 6. Raster Surface Volume Calculation in QGIS 3.44.6 Software



Figure 9

Figure 7. Aerial Photogrammetry for final validation